

1 **Routes for the electrochemical degradation of the**
2 **artificial food azo-colour Ponceau 4R by advanced**
3 **oxidation processes**

4 Abdoulaye Thiam, Enric Brillas, José A. Garrido, Rosa M. Rodríguez, Ignasi Sirés*

5 *Laboratori d'Electroquímica dels Materials i del Medi Ambient, Departament de Química Física,*

6 *Facultat de Química, Universitat de Barcelona, Martí i Franquès 1-11, 08028 Barcelona, Spain*

7 *Paper submitted to be published in Applied Catalysis B: Environmental*

8 * Corresponding author: Tel.: +34 934021223; fax: +34 934021231.

9 *E-mail address: i.sires@ub.edu (I. Sirés)*

11 **Abstract**

12 The performance of three electrochemical advanced oxidation processes, namely electro-
13 oxidation with electrogenerated H₂O₂ (EO-H₂O₂), electro-Fenton (EF) and photoelectro-Fenton
14 (PEF) for the treatment of aqueous solutions of the food azo dye Ponceau 4R in an undivided cell
15 with a BDD anode and an air-diffusion cathode was compared in terms of colour, dye concentration
16 and total organic carbon (TOC) removals. PEF treatments in ultrapure water with Na₂SO₄ were
17 performed to assess the effect of current density, as well as supporting electrolyte and dye
18 concentrations. At 100 mA cm⁻², solutions of 130 mL of 254 mg L⁻¹ of the dye in 0.05 M Na₂SO₄
19 became colourless and totally mineralized after 50 and 240 min, respectively, which can be
20 explained by the synergistic action of BDD(•OH) at the anode surface and homogeneous •OH
21 formed in the bulk from Fenton's reaction promoted in the presence of Fe²⁺ catalyst. Furthermore,
22 UVA photons induced the continuous Fe²⁺ regeneration and photolytic decomposition of refractory
23 intermediate complexes. In that aqueous matrix, the cleavage of the dye molecules proceeded
24 through several reaction routes to yield *N*-containing and non-*N*-containing derivatives with one or
25 two aromatic rings, short-chain aliphatic carboxylic acids and inorganic ions. Oxalic and oxamic
26 acids and sulfate ions were accumulated at different rates in EO-H₂O₂, EF and PEF. The three
27 methods allowed the progressive decontamination of Ponceau 4R solutions in a real water matrix
28 even without the addition of electrolyte, although complete TOC abatement after 360 min at 33.3
29 mA cm⁻² was only ensured by the iron-catalyzed PEF process.

30 *Keywords:* Acid Red 18; BDD anode; Catalyzed EAOPs; Food colours; Reaction pathways.

31

32 1. Introduction

33 Currently, food additives such as preservatives and colouring agents are among top food safety
34 concerns in industrialized countries, despite being carefully regulated by national and international
35 authorities. Indeed, their effects become uncontrolled when unintended targets, particularly children
36 or some highly sensitive person (HSP) with allergies or food intolerances, are routinely exposed to
37 them upon drinking water consumption. According to the International Food Information Council
38 (IFIC) and the US Food and Drug Administration (FDA), colour additives include dyes, pigments
39 and any other substance applied to a food, drug, cosmetic or the human body to impart colour [1].
40 Azo compounds are the most widespread synthetic colouring substances in the food industry, as
41 occurs in many other sectors [2,3], but the negative impact of the so-called food azo-colours has
42 been much less investigated than that of their textile counterparts so far. These dyes present one or
43 more azo (-N=N-) bonds and usually exhibit complex structures that confer them large stability
44 against physicochemical attack and bio/photodegradation, thus becoming persistent in water [3].

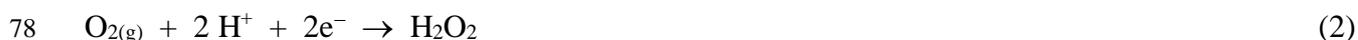
45 Ponceau 4R ($C_{20}H_{11}N_2O_{10}S_3Na_3$, trisodium 2-hydroxy-1-(4-sulphonato-1-naphthylazo)-
46 naphthalene-6,8-disulphonate, also known as Acid Red 18, New Coccine or additive E124 in the
47 industry, CI 16255, $\lambda_{max} = 508$ nm) is a paradigmatic case of sulphonated azo dyes employed to
48 give red colouring to foodstuffs. Lately, serious concerns have arisen since the intake of Ponceau
49 4R is plausibly connected to asthma and insomnia and it may increase children's hyperactivity and
50 intolerance [4]. As a result, in 2009, the European Food Safety Authority reduced the acceptable
51 daily intake from 4.0 to 0.7 mg (kg body weight)⁻¹ [5]. Despite being negative in *in vitro*
52 genotoxicity as well as in long-term carcinogenicity studies, the topic is still controversial [6]. For
53 instance, Ponceau 4R is currently not approved in the United States, Canada, Norway and Finland,
54 and it is listed as a banned substance by some authorities [7]. Since information about the safety of
55 water containing Ponceau 4R and other related azo dyes remains inconclusive [8], the best way to
56 reduce risks is to develop much more effective water treatment technologies that ensure their

57 complete removal before reaching end users. The great ability of advanced oxidation processes
58 (AOPs) such as heterogeneous photocatalysis [9,10], ozone-electrolysis with Pt anode [11],
59 chemical Fenton's reagent [12,13] and photo-Fenton [13] to degrade Ponceau 4R has been
60 demonstrated. For the two latter Fenton-based AOPs, however, scarce information was provided,
61 only describing a similar decolourization and mineralization rate in ultrapure water in both cases.
62 Note that those studies did not evaluate the possible influence of a more complex water matrix and
63 the formation of by-products, which is crucial for establishing the actual viability of both
64 techniques. Conversely, to the best of the authors' knowledge, the performance of the
65 electrochemical AOPs (EAOPs) to destroy this dye has not been reported yet.

66 In the last decade, considerable effort has been devoted to the study of fundamentals and scale-
67 up of electrochemical technologies for wastewater treatment, especially focusing on the destruction
68 of organic matter by hydroxyl radicals [14-16]. Electro-oxidation (EO) is the most popular EAOP
69 due to its simplicity, adaptability and outstanding performance of particular setups. This process
70 relies on the electrocatalytic properties of the anode surface (M), since some materials like Pt only
71 favour the partial conversion of contaminants by direct oxidation or under the action of
72 chemisorbed oxides (MO), whereas others like boron-doped diamond (BDD) may promote the
73 complete destruction of organic matter by physisorbed BDD(\bullet OH) formed as follows [17-23]:



75 The use of undivided cells with a BDD anode and an active cathode can enhance the degree
76 and/or rate of decontamination. Thus, in EO-H₂O₂, an air- or pure O₂-fed airtight or porous
77 carbonaceous cathode is employed to electrogenerate H₂O₂ as follows [24-28]:



79 H₂O₂ is a weak oxidant, although it can be oxidized to HO₂ \bullet at the anode or be further activated
80 in metal-catalyzed EAOPs like electro-Fenton (EF) and photoelectro-Fenton (PEF) [16]. In EF, the

81 presence of low amounts of Fe^{2+} leads to the production of $\bullet\text{OH}$ in the bulk through homogeneous
82 catalysis via Fenton's reaction (3) at optimum pH ~ 3 [29]. Organics are then destroyed upon the
83 synergistic action of heterogeneous and homogeneous catalysis (BDD($\bullet\text{OH}$) and $\bullet\text{OH}$, respectively).



85 If an UVA lamp is used to irradiate the solution in the EF setup, then so-called PEF process, the
86 mineralization is enhanced because UV photons induce the photoreduction of $\text{Fe}(\text{OH})^{2+}$ to Fe^{2+} via
87 reaction (4) and the photolysis of refractory Fe(III)-carboxylate products by reaction (5) [16,29].



90 BDD anode has an extraordinary oxidation power that favours the production of oxidants such
91 as H_2O_2 , O_3 , ferrate and peroxosalts ($\text{S}_2\text{O}_8^{2-}$, $\text{P}_2\text{O}_8^{4-}$ and $\text{C}_2\text{O}_6^{2-}$) depending on the aqueous matrix
92 composition [16]. When the treated acidic solution contains Cl^- ions, $\bullet\text{OH}$ and/or BDD($\bullet\text{OH}$) (and
93 UV in PEF) act in concomitance with active chlorine species (Cl_2 and HClO) produced in the bulk
94 via reactions (6) and (7) [3,14,16]. This medium, which is typical when treating real water matrices,
95 is quite complex since oxychlorine anions [30-32], (oxy)chlorine radicals [33], chloramines [34],
96 trihalomethanes and haloacetic acids [35], as well as refractory chlorinated by-products, can appear:



99 Encouraging results have been obtained for the treatment of textile azo dyes by EAOPs with a
100 BDD anode [36-40], and very recently we have even discussed the behaviour of two food azo dyes
101 in such systems [41,42]. In the present work, aiming to gain more thorough knowledge about the
102 fate of food azo-colours upon application of EAOPs, Ponceau 4R has been chosen as a model
103 pollutant. It has been comparatively degraded in EO- H_2O_2 , EF and PEF systems using an undivided
104 BDD/air-diffusion cell. Most electrolyses have been carried out in ultrapure water with added

105 Na₂SO₄ in order to investigate the effect of parameters like current density (*j*) and electrolyte and
106 pollutant contents on the colour, dye concentration, and total organic carbon (TOC) removals. The
107 reaction by-products identified by chromatographic techniques have allowed the proposal of various
108 reaction pathways. The viability of the tested EAOPs to degrade Ponceau 4R in a real water matrix
109 in the absence and presence of supporting electrolyte has been ascertained as well.

110 **2. Experimental**

111 *2.1. Chemicals*

112 Ponceau 4R (100% content) was purchased from Acros Organics. Anhydrous sodium sulfate,
113 sodium chloride and lithium perchlorate used as supporting electrolytes, as well as iron(II) sulfate
114 heptahydrate used as catalyst in EF and PEF, were of analytical grade supplied by Merck and Fluka.
115 Oxalic, oxamic, fumaric, tartaric, formic and maleic acids used as standards were of analytical
116 grade purchased from Merck, Avocado and Panreac. Sulfuric, hydrochloric and perchloric acids and
117 sodium hydroxide used to regulate the pH were of analytic grade purchased from Merck, Acros
118 Organics and Panreac. Organic solvents and other chemicals used were of high-performance liquid
119 chromatography (HPLC) or analytical grade supplied by Sigma-Aldrich, Lancaster, Merck and
120 Panreac. Solutions were prepared with ultrapure water obtained from a Millipore Milli-Q system
121 with resistivity >18 MΩ cm at 25 °C. Some comparative trials were also carried out with a real
122 water matrix collected from a secondary clarifier of a municipal wastewater treatment plant located
123 in Manresa (Barcelona, Spain). Its main characteristics determined in the laboratory were: pH 7.3,
124 specific conductivity = 1.9 mS cm⁻¹ (equivalent to ca. 0.010 M Na₂SO₄), TOC = 25 mg L⁻¹, 1.99
125 mM SO₄²⁻ and 10.3 mM Cl⁻. No iron ions were detected. This water was preserved at 4 °C and used
126 the day after collection.

127 *2.2. Electrochemical cells*

128 The experiments were conducted in an open, undivided, cylindrical glass tank reactor of 150
129 mL capacity equipped with a double jacket for recirculation of thermostated water at 25 °C. The
130 anode was a BDD thin-film electrode purchased from Adamant (at present, this material can be
131 acquired from NeoCoat or Waterdiam), whereas the cathode was a carbon-polytetrafluoroethylene
132 air-diffusion electrode purchased from E-TEK, mounted as described elsewhere [26] and fed with
133 compressed air pumped at 1 L min⁻¹ for continuous H₂O₂ generation from reaction (2). The
134 geometric area of each electrode was 3 cm² and the interelectrode gap was 1 cm. All experiments
135 were carried out using 130 mL of solutions at pH 3.0 under vigorous stirring with a magnetic bar at
136 800 rpm to ensure homogenization and the transport of reactants towards/from the electrodes. In EF
137 and PEF, 0.50 mM Fe²⁺ was employed as catalyst because this content was found optimal for
138 analogous treatments of aromatic azo dyes [16,29]. In PEF assays, the solution was irradiated with a
139 Philips TL/6W/08 fluorescent black light blue tube ($\lambda_{\text{max}} = 360$ nm, photoionization energy of 5 W
140 m⁻²) placed 7 cm above the solution. Before the assays, cleaning of the BDD anode and activation
141 of the air-diffusion electrode were achieved under polarization in 0.050 M Na₂SO₄ at 100 mA cm⁻²
142 for 180 min.

143 2.3. Apparatus and analytical procedures

144 The solution pH and the electrical conductance were measured with a Crison GLP 22 pH-meter
145 and a Metrohm 644 conductometer, respectively. Trials were carried out at constant j provided by
146 an EG&G PAR 273A potentiostat-galvanostat and the cell voltage was determined with a
147 Demestres 601BR digital multimeter. Samples withdrawn from electrolyzed solutions were
148 microfiltered with 0.45 μm PTFE filters purchased from Whatman prior to immediate analysis. The
149 decolourization of Ponceau 4R solutions was monitored by measuring their absorbance decay at
150 $\lambda_{\text{max}} = 508$ nm on a Shimadzu 1800 UV-Vis spectrophotometer at 25 °C. The mineralization of
151 solutions was assessed from their TOC abatement, determined on a Shimadzu TOC-VCNS

152 analyzer. Reproducible TOC values with an accuracy of $\pm 1\%$ were found by injecting 50 μL
153 aliquots into the analyzer.

154 The time course of the concentration of SO_4^{2-} and NO_3^- ions in trials in ultrapure water, as well
155 as Cl^- , ClO_3^- and ClO_4^- ions in trials in real water, was assessed by ion chromatography (IC) as
156 previously reported [43]. The decay of the dye concentration was followed by reversed-phase
157 HPLC using a Waters 600 LC fitted with a Thermo Scientific Hypersil ODS 5 μm , 150 mm \times 3
158 mm, column from Thermo Scientific at room temperature and coupled with a Waters 996
159 photodiode array detector set at $\lambda_{\text{max}} = 508$ nm. A 80:20 (v/v) acetonitrile/water (2.4 mM
160 butylamine) mixture at 0.2 mL min^{-1} was eluted as mobile phase. Generated carboxylic acids were
161 detected by ion-exclusion HPLC as described elsewhere [40].

162 Electrolytic experiments were made in triplicate with a good reproducibility of all the data.
163 Then, average results are given in all cases with standard deviations lower than 2%.

164 Well-defined peaks at characteristic retention times (t_r) were found in all cases: Cl^- (2.3 min),
165 ClO_3^- (3.4 min), NO_3^- (3.8 min), SO_4^{2-} (5.2 min) and ClO_4^- (15.2 min) ions by IC, Ponceau 4R (4.3
166 min) by reversed-phase HPLC, and oxalic (6.9 min), tartronic (7.9 min), oxamic (9.4 min) and
167 formic (13.7 min) acids by ion-exclusion HPLC.

168 Since only small traces of NH_4^+ ion, determined with a flow injection system [43], were found
169 in all the experiments, the theoretical number of electrons (n) exchanged per each substrate
170 molecule was taken as 102, assuming that Ponceau 4R is completely mineralized as follows:



172 The mineralization current efficiency (MCE) values for each trial at current I (in A) and time t
173 (in h) was then estimated as follows [37]:

$$174 \text{MCE (\%)} = \frac{(\Delta\text{TOC})_{\text{exp}} n F V_s}{4.32 \times 10^7 m I t} \times 100 \quad (9)$$

175 where F is the Faraday constant ($96,487 \text{ C mol}^{-1}$), V_s is the solution volume (in L), $\Delta(\text{TOC})_{\text{exp}}$ is the
176 experimental TOC abatement (in mg L^{-1}), 4.32×10^7 is a conversion factor to homogenize units (=
177 $3,600 \text{ s h}^{-1} \times 12,000 \text{ mg carbon mol}^{-1}$) and m is the number of carbon atoms of Ponceau 4R.

178 To identify the aromatic by-products, various samples were withdrawn during the electrolyses
179 and the organic components were extracted with CH_2Cl_2 ($3 \times 25 \text{ mL}$). In some cases, either
180 derivatization with acetic anhydride or ethanol, or liofilization followed by overnight derivatization,
181 were made prior to extraction. Each resulting organic solution was dried over anhydrous Na_2SO_4 ,
182 filtered and concentrated up to 1 mL under reduced pressure to be analyzed by gas chromatography-
183 mass spectrometry (GC-MS) using an Agilent Technologies system composed of a 6890N
184 chromatograph coupled to a 5975C spectrometer operating in EI mode at 70 eV. Nonpolar Agilent
185 J&W DB-5ms and polar HP INNOWax columns ($0.25 \mu\text{m}$, $30 \text{ m} \times 0.25 \text{ mm}$) were employed. The
186 temperature ramp was: $36 \text{ }^\circ\text{C}$ for 1 min, $5 \text{ }^\circ\text{C min}^{-1}$ up to $300 \text{ }^\circ\text{C}$ or $250 \text{ }^\circ\text{C}$ for the nonpolar and
187 polar columns, respectively, and hold time of 10 min. The temperature of the inlet, source and
188 transfer line was 250 , 230 and $280 \text{ }^\circ\text{C}$ for the nonpolar column, and 250 , 230 and $250 \text{ }^\circ\text{C}$ for the
189 polar one. The mass spectra were identified by comparison with those of a NIST05 MS library.

190 **3. Results and discussion**

191 *3.1. Electrochemical degradation of solutions of Ponceau 4R by PEF with a BDD anode*

192 The treatment of organic pollutants by PEF is known to yield much better results than EF and
193 EO- H_2O_2 , which is mainly due to the synergistic action of UVA photons that induce photochemical
194 reactions (4) and (5). Therefore, acidic solutions of 254 mg L^{-1} (0.42 mM) of Ponceau 4R in
195 ultrapure water with $0.05 \text{ M Na}_2\text{SO}_4$ as supporting electrolyte and 0.50 mM Fe^{2+} as catalyst were
196 treated by PEF until reaching total decolourization using a BDD/air-diffusion cell. The initial
197 solutions were bright red, as reported for other sulphonated monoazo dyes with two naphthalenes
198 like Acid Red 14 and Acid Red 88 employed to impart red colour to food and textiles, respectively

199 [41,44]. Fig. 1a shows the effect of applied j on the decay of normalized absorbance with
200 electrolysis time. Solutions became colourless after 70, 60, 50 and 40 min at 33.3, 66.7, 100 and
201 150 mA cm⁻², respectively. Higher current values are then beneficial in such system in terms of
202 time, since they promote both, the production of BDD([•]OH) from reaction (1) and H₂O₂ from
203 reaction (2) [37,41]. The quicker accumulation of the latter oxidant leads to a larger accumulation
204 of [•]OH in the bulk at a given time from reaction (3). Consequently, this radical species is the main
205 responsible for the fast colour removal in Fenton systems, thanks to the minimization of mass
206 transport limitations as compared to BDD([•]OH) that can only act in the anode vicinity. Note that the
207 enhancement obtained at 150 mA cm⁻² was not very significant if compared to 100 mA cm⁻². This
208 can be explained by the progressively lower current efficiency that results from: (i) the promoted
209 cathodic and anodic destruction of H₂O₂ and (ii) the BDD([•]OH) self-destruction to yield O₂ at
210 excessively high current values. Quite frequently in literature, colour removal trends are directly
211 associated to dye disappearance, but this is rarely verified because not enough attention is paid to
212 reaction intermediates. Fig. 1b depicts the decay of normalized dye concentration with time during
213 the same experiments. As found in Fig. 1a, a larger abatement was attained when j increased from
214 33.3 to 150 mA cm⁻², only requiring 40, 35, 30 and 25 min for total dye removal, respectively. This
215 confirms the great oxidizing ability of PEF system, but it also reveals the formation of coloured by-
216 products along the treatment because in all cases Ponceau 4R disappeared somewhat earlier than
217 colour. Such compounds were poorly concentrated and/or exhibited small molar extinction
218 coefficients. As shown in the inset panel of Fig. 1b, the concentration decays fitted very well to a
219 pseudo-first-order kinetics with $R^2 = 0.997$ and increasing apparent rate constants (k_{app} , 10⁻² min⁻¹)
220 of 11.39±1.74, 13.28±1.26, 16.76±0.96 and 18.60±2.56 as j was raised from 33.3 to 150 mA cm⁻²
221 (mean values along with their computed 95% confidence intervals are provided). The good linearity
222 can be accounted for by the accumulation of a constant concentration of hydroxyl radicals, both at
223 the anode and in the bulk, at each applied j .

224 The time course of normalized TOC for the previous trials is presented in Fig. 2a. A sigmoid
225 shape was observed in all cases, being the induction period more evident as j decreased. This is a
226 symptom of the formation of refractory by-products since the very beginning of the electrolysis,
227 which are slowly but progressively mineralized by BDD(\bullet OH) and \bullet OH. At high current, greater
228 concentrations of both oxidizing radicals are produced, thus accelerating the TOC abatement. For
229 example, TOC removals of 16%, 23%, 33% and 50% were obtained at 33.3, 66.7, 100 and 150 mA
230 cm^{-2} , respectively, after 60 min of electrolysis. The degradation by PEF at 150 mA cm^{-2} was
231 remarkably faster and, in fact, total mineralization was reached after only 180 min, whereas the
232 electrolyses at 33.3-100 mA cm^{-2} had to be prolonged for 240 min to completely remove the
233 organic matter (> 99% TOC reduction). Worth mentioning, the tail of the sigmoid curves that is
234 typical of mass transport limitation phenomena appeared at about $\text{TOC}_t/\text{TOC}_0 = 0.20$, which means
235 that gradual cleavage of Ponceau 4R (and/or its aromatic by-products) easily yielded CO_2 according
236 to mineralization reaction (8), but an unavoidable accumulation of persistent free and iron-
237 complexed by-products accounting for ca. 20% of TOC decelerated the degradation. Nonetheless,
238 the use of UVA light allowed the slow destruction of such refractory compounds over time. The
239 MCE values for the four experiments calculated from Eq. (9) are shown in Fig. 2b. As can be seen,
240 after a poorly efficient early stage related to the aforementioned induction period, maximum MCE
241 values of 55%, 29%, 21% and 18% were obtained after 90-120 min as current increased, whereupon
242 the efficiency decayed due to the accumulation of by-products that were highly resistant to
243 oxidation by BDD(\bullet OH) and \bullet OH and/or UVA photolysis. High current values are then preferred if
244 time is the key parameter for applying the treatment, whereas such choice is detrimental in terms of
245 energy consumption since parasitic reactions of BDD(\bullet OH) and \bullet OH are enhanced under such
246 conditions, especially as the organic matter content diminishes [37-42].

247 Considering the usual variability of wastewater composition regarding the electrolyte content, it
248 is interesting to investigate the effect of Na_2SO_4 concentration on PEF treatment. Fig. 3a shows the

249 normalized absorbance decay over time at 33.3 mA cm^{-2} when using $0.010\text{-}0.30 \text{ M Na}_2\text{SO}_4$. As can
250 be observed, total colour removal was always attained at 70 min. However, the extreme Na_2SO_4
251 concentration values yielded the quickest absorbance decays. It can then be deduced that 0.010 M
252 Na_2SO_4 is sufficient so as to confer the threshold conductivity that allows an efficient production of
253 BDD($\bullet\text{OH}$) and H_2O_2 at the anode and cathode, respectively. At that low SO_4^{2-} content, the parasitic
254 anodic generation of the weaker oxidant $\text{S}_2\text{O}_8^{2-}$ is considerably minimized, therefore giving
255 preponderance to the much more powerful BDD($\bullet\text{OH}$) [16]. Following this reasoning, a content as
256 high as $0.30 \text{ M Na}_2\text{SO}_4$ could seem largely detrimental, since part of BDD($\bullet\text{OH}$) is expected to be
257 wasted by the large formation of $\text{S}_2\text{O}_8^{2-}$ ion from the simultaneous SO_4^{2-} oxidation at the BDD
258 anode [14]. Conversely, the presence of large amounts of SO_4^{2-} ions entails a considerable increase
259 of the specific conductivity, which favours the transport of the negatively charged (sulphonated)
260 Ponceau 4R molecules towards the anode surface, eventually accelerating their oxidation. On the
261 other hand, Fig. 3b reveals that the effect of the Na_2SO_4 concentration on TOC removal was
262 negligible, leading to overlapped curves for 240 min. This can be justified by the conversion of
263 Ponceau 4R into non-ionic, more refractory compounds, whose mineralization takes place pre-
264 eminently in the solution bulk under the action of $\bullet\text{OH}$ from Fenton's reaction (3) and/or photolysis
265 by UVA photons from reaction (5). Our results then point to consider that the BDD anode plays an
266 important role during the initial decolourization steps, whereas Fenton's reaction and photolytic
267 reactions ensure the progressive TOC abatement.

268 The effect of initial dye concentration on its decolourization and mineralization trends was
269 examined for $127\text{-}1270 \text{ mg L}^{-1}$ of Ponceau 4R ($50\text{-}500 \text{ mg L}^{-1}$ TOC) in $0.050 \text{ M Na}_2\text{SO}_4$ with 0.50
270 mM Fe^{2+} at 100 mA cm^{-2} . Fig. 4a depicts the complete decay of normalized absorbance with
271 electrolysis time regardless of the dye content, which confirms the great oxidizing ability of PEF
272 with BDD. Increasing times of 20, 50, 70 and 240 min were needed as the dye concentration rose
273 from 127 to 1270 mg L^{-1} , which is simply due to the presence of larger amounts of coloured

274 compounds that must react with a constant quantity of BDD(\bullet OH) and \bullet OH. Worth noting, the PEF
275 treatment became more efficient as the organic matter content was raised. This behaviour arises
276 from the greater probability for favourable events in the presence of more organic molecules, thus
277 minimizing the parasitic reactions that involve BDD(\bullet OH) and \bullet OH. This can be more clearly seen
278 in the trends of normalized TOC over time collected in Fig. 4b. Total abatement with > 99% TOC
279 reduction was attained in all cases, needing longer times of 135, 240, 360 and 480 min for 127, 254,
280 635 and 1270 mg L⁻¹ of the dye, respectively. The MCE values for these trials depicted in Fig. 4c
281 show an increase in the efficiency for more concentrated dye solutions, especially at long
282 electrolysis time when the initial recalcitrant products were completely removed. Note that the TOC
283 profile obtained for the greatest dye content exhibits an evident shoulder (see Fig. 4b), which is
284 indicative of the progressively larger difficulties to remove the organic matter. This resulted in a
285 minimum MCE value at 120 min, although it further reached the highest efficiencies, which were
286 close to 35% at times > 240 min (see Fig. 4c). Several phenomena can be responsible for the
287 deceleration of degradation in Fenton systems at excessively high organic matter contents,
288 including iron complexation upon generation of many aliphatic by-products, polymerization and
289 partial blockage of the electrode surfaces that causes passivation [29].

290 3.2. Reaction by-products and proposed routes

291 As observed in Figs. 2a, 3b and 4b, the final stages of the PEF treatment were characterized by
292 a lower mineralization rate. This kind of behaviour has been usually associated to the formation of
293 polymers as well as short-chain carboxylic acids, whose absolute rate constants for their reaction
294 with hydroxyl radicals tends to be much smaller than those exhibited by aromatic compounds
295 [16,29]. In the present study, HPLC analyses of samples withdrawn from PEF experiments at 100
296 mA cm⁻² revealed the formation of up to 0.02 and 0.28 mM of tartronic and formic acids,
297 respectively, although they were easily mineralized under the action of BDD(\bullet OH) and \bullet OH
298 regardless of the formation of iron complexes [29]. A more particular situation was found for oxalic

299 and oxamic acids, whose concentration profiles with time are shown in [Figs. 5a](#) and [5b](#),
300 respectively. Oxalic acid was accumulated up to a maximum content of 0.45 mM at 60 min,
301 whereupon it gradually decayed up to its total disappearance at 180 min. A much smaller amount of
302 oxamic acid was formed, only reaching up to 0.014 mM at 90 min with total degradation at 210
303 min. These two findings agree with the mentioned high oxidizing ability of the PEF process with a
304 BDD anode (see the corresponding TOC evolution in [Fig. 2a](#)), which can then be justified by the
305 effective degradation of both acids and the Fe(II)-carboxylate complexes under the action of
306 BDD(\bullet OH) and \bullet OH, along with the efficient photodegradation of Fe(III)-oxalate and Fe(III)-
307 oxamate complexes by UVA photons [\[29\]](#). Clearly different profiles were obtained upon
308 comparative treatment of analogous Ponceau 4R solutions by EF and EO-H₂O₂ with a BDD anode,
309 which allowed the complete mineralization at 480 min but only 80% and 65% TOC removal at 240
310 min, respectively (not shown). In the former method, the maximum concentrations of oxalic and
311 oxamic acids were found at 90-120 min (0.88 and 0.012 mM, respectively, see [Fig. 5](#)). Due to the
312 large persistence of oxalic/oxalates, its total abatement was only ensured after 480 min of EF,
313 whereas oxamic acid disappeared at 270 min. This confirms the crucial role of UVA radiation,
314 which was responsible for the lower accumulation and faster removal in PEF. As reported
315 elsewhere, Fe(III)-oxalate complexes are quite refractory to \bullet OH formed in the bulk and thus, in EF,
316 only BDD(\bullet OH) is able to slowly oxidize them. On the other hand, very small amounts of oxalic (\leq
317 0.05 mM) and oxamic (\leq 0.005 mM) were detected in EO-H₂O₂, which can be explained by the
318 absence of iron complexes, therefore favouring the quick oxidation of all by-products by
319 BDD(\bullet OH). In conclusion, the extraordinary ability of PEF with BDD to quickly degrade both, the
320 parent pollutant and its coloured and colourless reaction by-products, allows explaining the superior
321 performance of this process as compared to the other EAOPs. Note that GC-MS analyses of treated
322 solutions allowed the identification of other aliphatic acids like maleic, fumaric, tartaric and

323 propanoic acids, which were not detected by ion-exclusion HPLC due to their quick removal and
324 very small accumulation.

325 Inorganic ions formed during the electrolyses were determined by IC. The N atoms forming the
326 -N=N- bond were preferentially detected as NO_3^- ion (50% of initial N) and, to a smaller extent, as
327 NH_4^+ ion (25%), as stated in reaction (8). A significant proportion of the initial N was then lost as
328 volatile nitrogenated products, like N_2 and N_xO_y , as reported for similar treatments of other azo
329 dyes [41,42,44]. Regarding the sulfur content, the initial S atoms were mainly released as SO_4^{2-} ion.
330 Fig. 6 depicts its time course during the degradation of 254 mg L^{-1} Ponceau 4R (0.42 mM) solutions
331 in 0.05 M LiClO_4 . As can be seen in Fig. 6a, in PEF, almost 1 mM SO_4^{2-} was accumulated after 50
332 min (80% of initial S). At that time, no coloured sulphonated by-products were present in the
333 solutions (see Fig. 1a), which means that S was contained in either sulphonated aliphatic
334 compounds or colourless aromatics. All of them were quickly oxidized and/or photolyzed and, at
335 the end of the treatment, ca. 100% of S (1.25 mM) was found as SO_4^{2-} . The trend of this ion was
336 analogous in EF, which means that UVA light mainly affects the non-sulphonated carboxylic acids,
337 as discussed above. A much slower accumulation was obtained in EO- H_2O_2 , only attaining the
338 expected SO_4^{2-} concentration after prolonged electrolysis. This confirms the great contribution of
339 $\bullet\text{OH}$ to mineralization, since its absence in the latter method yields lower degradation rates. On the
340 other hand, an increase in j from 33.3 to 150 mA cm^{-2} in PEF led to a faster accumulation of SO_4^{2-}
341 ions, as expected from the quicker generation of BDD($\bullet\text{OH}$) and $\bullet\text{OH}$ but, in all cases, this ion
342 accounted for the release of ca. 100% of S at the end of all the treatments.

343 Apart from revealing the formation of some additional aliphatic carboxylic acids, as mentioned
344 before, GC-MS analyses of treated solutions with polar and nonpolar columns allowed the
345 identification of nitromethane as well as various aromatic by-products. Their structures, chemical
346 names and characteristic m/z values have been gathered in Fig. 7, which constitutes a proposal of
347 different degradation routes for the electrolytic degradation of Ponceau 4R in acidic aqueous

348 medium by EO-H₂O₂, EF and PEF with a BDD anode. The final aliphatic intermediates formed
349 upon successive cleavage are also included.

350 Ponceau 4R appears with m/z 535, which corresponds to its anionic form without the sodium
351 counterions. Its degradation may proceed through the formation of up to six *N*-containing
352 derivatives (highlighted in green) following four different routes (A-D). A, B and C inform about
353 the appearance of four *N*-based heterocycles, which can be plausibly produced upon primary radical
354 formation from electron transfer at the cathode (so-called electrochemically-induced radical
355 cyclization [45]). Path A involves intramolecular cyclization, path B arises from intermolecular
356 cyclization as suggested by the presence of an additional carbon to close the *N*-cycle and path C
357 comes from intra or intermolecular cyclization because some of the carbon atoms of benzene might
358 allow closing the *N*-cycle. Among all the heterocycles, phthalimide was the most ubiquitous one.
359 Conversely, route D leads to two aromatic amines, which were typically formed when a stainless
360 steel cathode was used instead of the air-diffusion electrode, thus confirming the purely oxidative
361 degradation underwent by the azo dye in systems with BDD/air-diffusion cells.

362 Alternatively, Ponceau 4R can follow route E to yield up to twelve non-*N*-containing
363 derivatives (highlighted in blue) with one or two cycles, starting with its conversion to α -naphthol.
364 As observed, this compound is the source of most of these by-products, except indandione, via 1,4-
365 naphthoquinone. Discontinuous arrows account for transformations that can take place or rather be
366 GC-MS artifacts, being impossible to elucidate the exact by-product in each case. Ponceau 4R, as
367 well as its eighteen aromatic by-products, can be further transformed into non-*N*-containing
368 derivatives with one cycle, such as resorcinol, acetophenone and their hydroxylated by-products
369 following route F (highlighted in pink). Worth mentioning, a condensation reaction involving
370 acetophenone could potentially yield indandione, as occurs in well-known aldol condensation. The
371 cleavage of any of the 22 aromatic structures caused the formation of aliphatic compounds, which
372 were finally mineralized to CO₂ under optimized electrolysis conditions.

373 Some of the intermediates proposed in this work are consistent with those obtained during the
374 degradation of other azo dyes. For example, the treatment of Acid Orange 7, which includes a
375 phenylazonaphthol group, by TiO₂ photocatalysis yielded naphthol, naphthalene-1,4-diol, 1,4-
376 naphthoquinone, hydroxynaphthoquinone, phthalic anhydride, 3*H*-isobenzofuran-1-one (phthalide)
377 and phthalimide [46].

378 3.3. Treatments with a BDD anode in a real water matrix

379 The great performance of EAOPs with a BDD anode, particularly PEF, regarding the
380 decontamination of acidic Ponceau 4R solutions has been demonstrated for pure water matrices.
381 However, real dye wastewater is not so ideal because it usually contains natural organic matter and
382 various inorganic anions, which may hamper the application of those technologies. Therefore, some
383 experiments were carried out using a real water matrix (see section 2.1). First, the raw real water
384 samples (TOC = 25 mg L⁻¹) were treated at 25 °C and 33.3 mA cm⁻² in the absence of the dye by
385 EO-H₂O₂, EF and PEF. Prior to the electrolyses, the initially alkaline pH was adjusted to 3.0, and
386 0.50 mM Fe²⁺ was added to the solutions for the two latter treatments. The time course of natural
387 TOC with time is shown in Fig. 8a. EO-H₂O₂ allowed a significant TOC abatement thanks to the
388 action of BDD([•]OH) on organic matter, eventually reaching 86% mineralization at 360 min. TOC
389 removal was accelerated in EF from the beginning of the treatment, with > 95% mineralization at
390 360 min. This suggests that the catalytic amount of Fe²⁺ favours the formation of [•]OH during all the
391 electrolysis, notwithstanding the plausible partial complexation of iron ions by chelating species
392 contained in the water sample. The rate and degree of mineralization was very similar in the case of
393 PEF process, which means that photosensitive Fe(III) complexes such as Fe(III)-oxalate species
394 were not formed to a large extent along the treatment.

395 Since the water sample contained about 2.0 mM SO₄²⁻ and 10.3 mM Cl⁻, some oxychlorine
396 anions were formed under the oxidative action of BDD, BDD([•]OH) and [•]OH [30-32]. As an
397 example, the evolution of chlorinated ions in PEF process is illustrated in Fig. 8b. The Cl⁻

398 concentration gradually decreased to 3.4 mM at 360 min, owing to its transformation into ClO_3^-
399 (3.6 mM) and ClO_4^- (3.3 mM) ions. As can be observed, such conversion was quite quantitative
400 because the sum of the three anions accounted for almost 100% of the initial Cl content. This
401 suggests a very small accumulation of active chlorine from reactions (6) and (7) and therefore, the
402 mineralization of organic matter in Fig. 8a can be essentially explained by the participation of
403 hydroxyl radicals. Furthermore, the accumulation of Cl in the form of chlorinated anions ensures
404 that the generation of toxic chlorinated organic by-products during the treatment can be neglected.

405 The performance of the three EAOPs during the degradation of 254 mg L^{-1} of Ponceau 4R in
406 the same real water matrix of Fig. 8, at pH 3.0 and 33.3 mA cm^{-2} , was further assessed. Fig. 9a
407 presents the decay of the normalized absorbance achieved by EO- H_2O_2 , EF and PEF in the absence
408 or presence of added electrolyte. When treating the dye in the raw water, total colour removal was
409 attained after 180, 100 and ca. 70 min, respectively, in agreement with the higher oxidizing ability
410 in the sequence $\text{EO-H}_2\text{O}_2 < \text{EF} < \text{PEF}$. Note that the time needed in PEF is similar to that found in
411 Fig. 1a for the treatment under analogous conditions but using ultrapure water, which means that
412 the water matrix does not impede the fast decolourization of the dye solutions. Actually, the real
413 matrix was even beneficial, since 50% colour removal was reached after 10-15 min of PEF instead
414 of 25 min required in ultrapure water (see Fig. 1a). This suggests the contribution of active chlorine
415 to the oxidation of coloured compounds, despite the very small accumulation of such oxidant (see
416 Fig. 8b). The participation of active chlorine was more evident when the PEF treatment was
417 performed in the presence of 0.010 M NaCl , which allowed a quicker decolourization with total
418 disappearance of coloured compounds at 60 min. In contrast, the addition of $0.010 \text{ M Na}_2\text{SO}_4$ did
419 not enhance the process, but it was slightly detrimental by the formation of competitive $\text{S}_2\text{O}_8^{2-}$ ion.

420 The decay of the normalized dye concentration for the experiments of Fig. 9a without added
421 electrolyte is shown in Fig. 9b, along with the corresponding kinetic analysis assuming a pseudo-
422 first-order reaction. Ponceau 4R disappeared after 140 min in EO- H_2O_2 , only requiring about 40

423 min in EF and PEF, thus confirming the superiority of Fenton processes due to the much faster
424 reaction of the azo dye with $\bullet\text{OH}$ formed from Fenton's reaction (3). The mean values of k_{app} (10^{-2}
425 min^{-1}) with their 95% confidence intervals were 2.72 ± 0.41 , 12.31 ± 0.53 and 13.35 ± 0.66 for EO-
426 H_2O_2 , EF and PEF, respectively. As also observed in Fig. 1, the time needed for removing the dye
427 was lower than that for colour removal. Note that Ponceau 4R disappeared at the same time in both,
428 ultrapure (see Fig. 1b) and real water matrices (see Fig. 9b), indicating a small participation of
429 active chlorine.

430 Finally, Fig. 9c shows the TOC removal during all the trials of Fig. 9a. At 360 min, 57%, 74%
431 and $\sim 100\%$ mineralization was attained by EO- H_2O_2 , EF and PEF, respectively. This result, along
432 with the fast colour and Ponceau 4R removals, verifies the viability of PEF process for the
433 treatment of real wastewater. Comparison with the TOC abatement in ultrapure water (see Fig. 2a),
434 where total mineralization was reached after 240 min, allowed concluding that the degradation
435 proceeded somewhat more slowly, with 93% TOC decay at that time. This can be explained by: (i)
436 the presence of a larger amount of organic matter due to the natural constituents, (ii) the partial
437 consumption of BDD($\bullet\text{OH}$) by Cl^- to form less oxidizing species [30-33], (iii) the partial
438 destruction of H_2O_2 by HClO formed via reactions (6) and (7) [32] and (iv) the formation of chloro-
439 complexes that reduce the amount of free iron ions [47]. While the presence of Cl^- resulted positive
440 for colour removal (see Fig. 9a), it became detrimental regarding the TOC abatement. This was
441 confirmed when treating the dye in the presence of 0.010 M NaCl , since only 82% and 92%
442 mineralization could be attained after 240 and 360 min of PEF, respectively. In contrast, the effect
443 of added Na_2SO_4 was insignificant, as discussed above.

444 4. Conclusions

445 Iron-catalyzed PEF treatment using a BDD/air-diffusion cell has been proven a promising
446 technology for the degradation of food azo-colours like Ponceau 4R contained in real water

447 matrices thanks to the synergistic action of BDD(\bullet OH), \bullet OH and UVA photons. No significant
448 detrimental effects of the real matrix were observed, since the time required for the complete dye
449 and colour removals was comparable to that needed in ultrapure water, whereas only a slight
450 deceleration of TOC decay was revealed as a result of parasitic reactions induced by the presence of
451 Cl^- . Up to 22 aromatic by-products, 8 carboxylic acids and nitromethane were identified upon
452 treatment of Ponceau 4R by EAOPs with BDD. The total mineralization of all these by-products to
453 yield CO_2 , NO_3^- , NH_4^+ and SO_4^{2-} proceeded via various simultaneous reaction routes.

454 **Acknowledgments**

455 The authors thank MINECO (Ministerio de Economía y Competividad, Spain) for financial
456 support under project CTQ2013-48897-C2-1-R, co-financed with FEDER funds. The Ph.D. grant
457 awarded to A. Thiam from MAEC-AECID (Spain) is also acknowledged.

458 **References**

- 459 [1] IFIC and FDA, Food ingredients and colors, pp. 1-7
460 (<http://www.fda.gov/downloads/Food/IngredientsPackagingLabeling/ucm094249.pdf>;
461 November 2004, revised April 2010).
- 462 [2] I.K. Konstantinou, T.A. Albanis, *Appl. Catal. B: Environ.* 49 (2004) 1-14.
- 463 [3] E. Brillas, C.A. Martínez-Huitle, *Appl. Catal. B: Environ.* 166-167 (2015) 603-643.
- 464 [4] D. McCann, A. Barrett, C. Cooper, D. Crumpler, L. Dalen, K. Grimshaw, E. Kitchin, K. Lok,
465 L. Porteous, E. Prince, E. Sonuga-Barke, J. O'Warner, J. Stevenson, *Lancet* 370 (2007) 1560-
466 1567.
- 467 [5] EFSA, *EFSA J.* 7 (2009) 1328-1366.
- 468 [6] L.E. Arnold, N. Lofthouse, E. Hurt, *Neurotherapeutics* 9 (2012) 599-609.
- 469 [7] <http://www.fda.gov/ForIndustry/ColorAdditives/ColorAdditiveInventories/ucm115641.htm>
- 470 [8] M.M. Ghoneim, H.S. El-Desoky, N.M. Zidan, *Desalination* 274 (2011) 22-30.
- 471 [9] K. Tanaka, K. Padermpole, T. Hisanaga, *Water Res.* 34 (2000) 327-333.
- 472 [10] N. Sobana, M. Swaminathan, *Sep. Purif. Technol.* 56 (2007) 101-107.
- 473 [11] J. Basiri Parsa, M. Golmirzaei, M. Abbasi, *J. Ind. Eng. Chem.* 20 (2014) 689-694.
- 474 [12] K. Barbusiński, J. Majewski, *Pol. J. Environ. Studies* 12 (2003) 151-155.
- 475 [13] C. Benincá, P. Peralta-Zamora, R.C. Camargo, C.R.G. Tavares, E.F. Zanoelo, L. Igarashi-
476 Mafra, *Reac. Kinet. Mech. Cat.* 105 (2012) 293-306.
- 477 [14] M. Panizza, G. Cerisola, *Chem. Rev.* 109 (2009) 6541-6569.
- 478 [15] B.P. Chaplin, *Environ. Sci. Process. Impacts* 16 (2014) 1182-1203.
- 479 [16] I. Sirés, E. Brillas, M.A. Oturan, M.A. Rodrigo, M. Panizza, *Environ. Sci. Pollut. Res.* 21
480 (2014) 8336-8367.
- 481 [17] L. Ciríaco, C. Anjo, J. Correia, M.J. Pacheco, A. Lopes, *Electrochim. Acta* 54 (2009) 1464-
482 1472.

- 483 [18] M.A. Rodrigo, P. Cañizares, A. Sánchez-Carretero, C. Sáez, *Catal. Today* 151 (2010) 173-
484 177.
- 485 [19] A. El-Ghenymy, F. Centellas, J.A. Garrido, R.M. Rodríguez, I. Sirés, P.L. Cabot, E. Brillas,
486 *Electrochim. Acta* 130 (2014) 568-576.
- 487 [20] M. Panizza, *Environ. Sci. Pollut. Res.* 21 (2014) 8451-8456.
- 488 [21] O. Scialdone, E. Corrado, A. Galia, I. Sirés, *Electrochim. Acta* 132 (2014) 15-24.
- 489 [22] M.J.M.D. Vidales, S. Barba, C. Sáez, P. Cañizares, M.A. Rodrigo, *Electrochim. Acta* 140
490 (2014) 20-26.
- 491 [23] D.M.D. Araújo, C. Sáez, C.A. Martínez-Huitle, P. Cañizares, M.A. Rodrigo, *Appl. Catal. B:*
492 *Environ.* 166-167 (2015) 454-459.
- 493 [24] A. Özcan, Y. Sahin, A.S. Koparal, M.A. Oturan, *J. Electroanal. Chem.* 616 (2008) 71-78.
- 494 [25] E. Rosales, M. Pazos, M.A. Longo, M.A. Sanromán, *Chem. Eng. J.* 155 (2009) 62-67.
- 495 [26] E. Guinea, J.A. Garrido, R.M. Rodríguez, P.L. Cabot, C. Arias, F. Centellas, E. Brillas,
496 *Electrochim. Acta* 55 (2010) 2101-2115.
- 497 [27] M. Panizza, M.A. Oturan, *Electrochim. Acta* 56 (2011) 7084-7087.
- 498 [28] A. Dirany, I. Sirés, N. Oturan, A. Özcan, M.A. Oturan, *Environ. Sci. Technol.* 46 (2012)
499 4074-4082.
- 500 [29] E. Brillas, I. Sirés, M.A. Oturan, *Chem. Rev.* 109 (2009) 6570-6631.
- 501 [30] M.E. Bergmann, J. Rollin, *Catal. Today* 124 (2007) 198-203.
- 502 [31] A.M. Polcaro, A. Vacca, M. Mascia, S. Palmas, J. Rodriguez Ruiz, *J. Appl. Electrochem.* 39
503 (2009) 2083-2092.
- 504 [32] S. Randazzo, O. Scialdone, E. Brillas, I. Sirés, *J. Hazard. Mater.* 192 (2011) 1555-1564.
- 505 [33] F. Bonfatti, S. Ferro, F. Lavezzo, M. Malacarne, G. Lodi, A. De Battisti, *J. Electrochem. Soc.*
506 147 (2000) 592-596.
- 507 [34] M. Deborde, U. von Gunten, *Water Res.* 42 (2008) 13-51.

- 508 [35] S.D. Richardson, *Global NEST J.* 7 (2005) 43-60.
- 509 [36] M. Panizza, G. Cerisola, *Ind. Eng. Chem. Res.* 47 (2008) 6816-6820.
- 510 [37] E.J. Ruiz, C. Arias, E. Brillas, A. Hernández-Ramírez, J.M. Peralta-Hernández, *Chemosphere*
511 82 (2011) 495-501.
- 512 [38] L.C. Almeida, S. Garcia-Segura, C. Arias, N. Bocchi, E. Brillas, *Chemosphere* 89 (2012) 751-
513 758.
- 514 [39] R., Salazar, E. Brillas, I. Sirés, *Appl. Catal. B: Environ.* 115–116 (2012) 107-116.
- 515 [40] F.C. Moreira, S. Garcia-Segura, V.J.P. Vilar, R.A.R. Boaventura, E. Brillas, *Appl. Catal. B:*
516 *Environ.* 142-143 (2013) 877-890.
- 517 [41] A. Thiam, I. Sirés, J.A. Garrido, R.M. Rodríguez, E. Brillas, *Sep. Purif. Technol.* 140 (2015)
518 43-52.
- 519 [42] A Thiam, I. Sirés, J.A. Garrido, R.M. Rodríguez, E. Brillas, *J. Hazard. Mater.* 290 (2015) 34-
520 42.
- 521 [43] A.R.F. Pipi, A.R. De Andrade, E. Brillas, I. Sirés, *Sep. Purif. Technol.* 132 (2014) 674-683.
- 522 [44] E.J. Ruiz, A. Hernández-Ramírez, J.M. Peralta-Hernández, C. Arias, E. Brillas, *Chem. Eng. J.*
523 171 (2011) 385-392.
- 524 [45] S. Donnelly, J. Grimshaw, J. Trocha-Grimshaw, *Electrochim. Acta* 41 (1996) 489-492.
- 525 [46] M. Styliidi, D.I. Kondarides, X.E. Verykios, *Appl. Catal. B: Environ.* 40 (2003) 271-286.
- 526 [47] J. De Laat, G.T. Le, B. Legube, *Chemosphere* 55 (2004) 715-723.

527

528 **Figure captions**

529 Fig. 1. Effect of applied current on the decay of the (a) normalized absorbance at 508 nm and (b)
530 normalized dye concentration with electrolysis time for the degradation of 130 mL of a 254 mg L⁻¹
531 (= 0.42 mM) of Ponceau 4R solution in 0.050 M Na₂SO₄ at pH 3.0 and 25 °C by photoelectro-
532 Fenton (PEF) process in the presence of 0.50 mM Fe²⁺ as catalyst. The cell contained a 3 cm² BDD
533 anode and a 3 cm² air-diffusion cathode and the solution was irradiated with a 6 W UVA lamp of
534 $\lambda_{\text{max}} = 360$ nm. Current density: (○) 33.3 mA cm⁻², (□) 66.7 mA cm⁻², (△) 100 mA cm⁻² and (◇)
535 150 mA cm⁻².

536 Fig. 2. Change of: (a) normalized TOC and (b) mineralization current efficiency with electrolysis
537 time for the trials shown in Fig. 1.

538 Fig. 3. Effect of supporting electrolyte concentration on the (a) normalized absorbance decay at 508
539 nm and (b) normalized TOC abatement vs electrolysis time for the degradation of 130 mL of 254
540 mg L⁻¹ of Ponceau 4R solutions in: (○) 0.010 M, (□) 0.050 M, (△) 0.15 M and (◇) 0.30 M
541 Na₂SO₄ with 0.50 mM Fe²⁺ at pH 3.0 and 25 °C by PEF with a BDD anode at 33.3 mA cm⁻².

542 Fig. 4. Effect of dye concentration on the (a) normalized absorbance at 508 nm, (b) normalized
543 TOC decay and (c) mineralization current efficiency with electrolysis time for the degradation of
544 130 mL of: (○) 127 mg L⁻¹, (□) 254 mg L⁻¹, (△) 635 mg L⁻¹ and (◇) 1270 mg L⁻¹ of Ponceau 4R
545 solutions in 0.050 M Na₂SO₄ with 0.50 mM Fe²⁺ at pH 3.0 and 25 °C by PEF with a BDD anode at
546 100 mA cm⁻².

547 Fig. 5. Evolution of the concentration of (a) oxalic and (b) oxamic acids detected during the
548 degradation of 130 mL of 254 mg L⁻¹ of Ponceau 4R solutions in 0.050 M Na₂SO₄ at pH 3.0, 25 °C
549 and 100 mA cm⁻². Methods with a BDD anode: (○) EO-H₂O₂, (□) EF with 0.50 mM Fe²⁺ and (△)
550 PEF with 0.50 mM Fe²⁺.

551 Fig. 6. Time course of the concentration of SO_4^{2-} ions released during the degradation of 130 mL of
552 254 mg L^{-1} of Ponceau 4R solutions in 0.050 M LiClO_4 at pH 3.0 and $25 \text{ }^\circ\text{C}$ with a BDD anode. In
553 (a), (\circ) EO- H_2O_2 , (\square) EF with 0.50 mM Fe^{2+} and (\triangle) PEF with 0.50 mM Fe^{2+} at 100 mA cm^{-2} . In
554 (b), PEF with 0.5 mM Fe^{2+} at: (\circ) 33.3 mA cm^{-2} , (\triangle) 100 mA cm^{-2} and (\diamond) 150 mA cm^{-2} .

555 Fig. 7. Routes for the electrolytic degradation of Ponceau 4R in acidic aqueous medium by EAOPs
556 with BDD anode. The primary oxidation by-products, as well as some of the final aliphatic
557 intermediates, were identified by GC-MS.

558 Fig. 8. Performance of the EAOPs with a BDD anode during the treatment of 130 mL of a real
559 water sample at pH 3.0, $25 \text{ }^\circ\text{C}$ and 33.3 mA cm^{-2} . (a) TOC removal by (\circ) EO- H_2O_2 , (\square) EF with
560 0.50 mM Fe^{2+} and (\triangle) PEF with 0.50 mM Fe^{2+} . (b) Time course of the concentration of chlorinated
561 ions accumulated in PEF process. (\circ) Cl^- , (\square) ClO_3^- , (\triangle) ClO_4^- and (\diamond) sum of chlorinated ions.

562 Fig. 9. Performance of the EAOPs with a BDD anode during the degradation of 130 mL of 254 mg
563 L^{-1} of Ponceau 4R in the same real water matrix of Fig. 8, at pH 3.0, $25 \text{ }^\circ\text{C}$ and 33.3 mA cm^{-2} . (a)
564 Decay of the normalized absorbance at 508 nm without added electrolyte by (\circ) EO- H_2O_2 , (\square) EF
565 with 0.50 mM Fe^{2+} and (\triangle) PEF with 0.50 mM Fe^{2+} , and with addition of (\bullet) $0.010 \text{ M Na}_2\text{SO}_4$ or
566 (\blacksquare) 0.010 M NaCl in PEF. (b) Decay of the normalized dye concentration in the experiments
567 without added electrolyte. (c) TOC removal during the trials shown in plot (a).